



UvA-DARE (Digital Academic Repository)

Integrated post-genomic cell wall analysis reveals floating biofilm formation associated with high expression of flocculins in the pathogen *Pichia kudriavzevii*

Alvarado, M.; Gómez-Navajas, J.A.; Blázquez-Muñoz, M.T.; Gómez-Molero, E.; Berbegal, C.; Eraso, E.; Kramer, G.; De Groot, P.W.J.

DOI

[10.1371/journal.ppat.1011158](https://doi.org/10.1371/journal.ppat.1011158)

Publication date

2023

Document Version

Final published version

Published in

PLoS Pathogens

License

CC BY

[Link to publication](#)

Citation for published version (APA):

Alvarado, M., Gómez-Navajas, J. A., Blázquez-Muñoz, M. T., Gómez-Molero, E., Berbegal, C., Eraso, E., Kramer, G., & De Groot, P. W. J. (2023). Integrated post-genomic cell wall analysis reveals floating biofilm formation associated with high expression of flocculins in the pathogen *Pichia kudriavzevii*. *PLoS Pathogens*, 19(5), Article e1011158. <https://doi.org/10.1371/journal.ppat.1011158>

General rights

It is not permitted to download or to forward/distribute the text or part of it without the consent of the author(s) and/or copyright holder(s), other than for strictly personal, individual use, unless the work is under an open content license (like Creative Commons).

Disclaimer/Complaints regulations

If you believe that digital publication of certain material infringes any of your rights or (privacy) interests, please let the Library know, stating your reasons. In case of a legitimate complaint, the Library will make the material inaccessible and/or remove it from the website. Please Ask the Library: <https://uba.uva.nl/en/contact>, or a letter to: Library of the University of Amsterdam, Secretariat, P.O. Box 19185, 1000 GD Amsterdam, The Netherlands. You will be contacted as soon as possible.
UvA-DARE is a service provided by the library of the University of Amsterdam (<https://dare.uva.nl>)

RESEARCH ARTICLE

Integrated post-genomic cell wall analysis reveals floating biofilm formation associated with high expression of flocculins in the pathogen *Pichia kudriavzevii*

María Alvarado¹, Jesús Alberto Gómez-Navajas¹, María Teresa Blázquez-Muñoz¹, Emilia Gómez-Molero¹, Carmen Berbegal², Elena Eraso³, Gertjan Kramer⁴, Piet W. J. De Groot^{1*}

1 Regional Center for Biomedical Research, Castilla-La Mancha Science & Technology Park, University of Castilla-La Mancha, Albacete, Spain, **2** ENOLAB, Estructura de Recerca Interdisciplinar (ERI) BioTecMed and Departament de Microbiologia i Ecologia, Universitat de València, Burjassot, Spain, **3** Department of Immunology, Microbiology and Parasitology, Faculty of Medicine and Nursing, University of the Basque Country (UPV/EHU), Bilbao, Spain, **4** Mass Spectrometry of Biomolecules, University of Amsterdam, Swammerdam Institute for Life Sciences Amsterdam, Amsterdam, The Netherlands

* piet.degroot@uclm.es



OPEN ACCESS

Citation: Alvarado M, Gómez-Navajas JA, Blázquez-Muñoz MT, Gómez-Molero E, Berbegal C, Eraso E, et al. (2023) Integrated post-genomic cell wall analysis reveals floating biofilm formation associated with high expression of flocculins in the pathogen *Pichia kudriavzevii*. PLoS Pathog 19(5): e1011158. <https://doi.org/10.1371/journal.ppat.1011158>

Editor: Alex Andrianopoulos, University of Melbourne, AUSTRALIA

Received: January 27, 2023

Accepted: April 27, 2023

Published: May 17, 2023

Copyright: © 2023 Alvarado et al. This is an open access article distributed under the terms of the [Creative Commons Attribution License](https://creativecommons.org/licenses/by/4.0/), which permits unrestricted use, distribution, and reproduction in any medium, provided the original author and source are credited.

Data Availability Statement: The raw proteomic data has been submitted to ProteomeXchange (accession number PXD041801) through the MassIVE partner repository.

Funding: This work was supported by grants SBPLY/19/180501/000114 (JG, MB, EE, PG) and SBPLY/19/180501/000356 (MA) funded by the Regional Government of Castilla-La Mancha grants SAF2017-86188-P (EE, PG), and PID2020-

Abstract

The pathogenic yeast *Pichia kudriavzevii*, previously known as *Candida krusei*, is more distantly related to *Candida albicans* than clinically relevant CTG-clade *Candida* species. Its cell wall, a dynamic organelle that is the first point of interaction between pathogen and host, is relatively understudied, and its wall proteome remains unidentified to date. Here, we present an integrated study of the cell wall in *P. kudriavzevii*. Our comparative genomic studies and experimental data indicate that the general structure of the cell wall in *P. kudriavzevii* is similar to *Saccharomyces cerevisiae* and *C. albicans* and is comprised of β -1,3-glucan, β -1,6-glucan, chitin, and mannoproteins. However, some pronounced differences with *C. albicans* walls were observed, for instance, higher mannan and protein levels and altered protein mannosylation patterns. Further, despite absence of proteins with high sequence similarity to *Candida* adhesins, protein structure modeling identified eleven proteins related to flocculins/adhesins in *S. cerevisiae* or *C. albicans*. To obtain a proteomic comparison of biofilm and planktonic cells, *P. kudriavzevii* cells were grown to exponential phase and in static 24-h cultures. Interestingly, the 24-h static cultures of *P. kudriavzevii* yielded formation of floating biofilm (flor) rather than adherence to polystyrene at the bottom. The proteomic analysis of both conditions identified a total of 33 cell wall proteins. In line with a possible role in flor formation, increased abundance of flocculins, in particular Flo110, was observed in the floating biofilm compared to exponential cells. This study is the first to provide a detailed description of the cell wall in *P. kudriavzevii* including its cell wall proteome, and paves the way for further investigations on the importance of flor formation and flocculins in the pathogenesis of *P. kudriavzevii*.

117983RB-I00 (MA, MB, EE, PG) funded by MCIN/AEI/10.13039/501100011033 and by European Regional Development Fund (ERDF), a way of making Europe. The funders had no role in study design, data collection and analysis, decision to publish, or preparation of the manuscript.

Competing interests: The authors have declared that no competing interests exist.

Author summary

The yeast *P. kudriavzevii* (ex-*Candida krusei*) is among the five most prevalent causal agents of candidiasis but its mechanisms underlying pathogenicity have been scarcely studied. This is also true for its cell wall structure, an essential organelle that governs primary host-pathogen interactions and host immune responses. Solid knowledge about cell wall synthesis and dynamics is crucial for the development of novel antifungal strategies against this pathogenic yeast. Here, through a combination of comparative genomics, protein structure modeling, and biochemical and proteomic analysis of purified walls, we present a detailed study of the cell wall composition in *P. kudriavzevii* and identify important architectural differences compared to *C. albicans* cell walls. Cell walls of *P. kudriavzevii* contain higher mannan and protein levels with altered mannan branching patterns, governed by expansions and reductions in gene families encoding mannosyltransferases. We also show that, in contrast to other *Candida* species, static cultures produce floating biofilms. Comparative wall proteomic studies of these biofilms show increased abundance of flocculins and hydrolytic enzymes, protein classes implicated in biofilm formation and primary host-pathogen interactions leading to tissue colonization. In conclusion, our study uncovers important keys towards a better molecular understanding of the virulence mechanisms of the important pathogen *P. kudriavzevii*.

Introduction

Candidiasis is one of the most frequent fungal infections in humans. In immunocompromised patients *Candida* infections frequently lead to invasive mycoses or bloodstream infections (candidemia), which are associated with high mortality rates [1]. *Pichia kudriavzevii* (ex-*Candida krusei*), is among the most relevant etiological agents of candidiasis and is most often found in patients with hematological malignancies or receiving prolonged azole prophylaxis [2, 3]. Infections caused by this organism are of special clinical relevance because of its intrinsic resistance to fluconazole [4].

P. kudriavzevii is a diploid ascomycete yeast belonging to the family *Pichiaceae* in the order Saccharomycetales. It does not belong to the *Candida*-CTG clade [5] and is only distantly related to *Candida albicans* [4, 6]. Recently, it has been suggested that the commonly used name of this pathogenic yeast, *C. krusei*, should be changed to the more accurate name of its environmental teleomorph, *P. kudriavzevii*, which will be more informative for clinicians [7].

Among the virulence factors described for *P. kudriavzevii*, there are similarities with *Candida* spp., for instance, formation of pseudohyphae that would confer the ability to invade host tissues [8], secretion of phospholipases and proteinases that enhance the yeast ability to colonize host tissues and evade the host immune system [9], phenotypic switching contributing to its adaptation to environmental conditions [10], or formation of monospecies or polymicrobial biofilms [11].

Playing a key role in primary host-pathogen interactions, the fungal cell wall is crucial for all the aforementioned virulence mechanisms [12, 13]. In related yeasts such as *Saccharomyces cerevisiae* and *C. albicans*, the inner part of the cell wall has been described as a carbohydrate network mostly composed of the polysaccharides β -1,3-glucan, β -1,6-glucan and chitin, whereas the outer cell wall layer is densely packed with highly glycosylated (mostly by mannosyl residues) glycosylphosphatidylinositol (GPI)-modified proteins that are covalently bound to β -1,6-glucan molecules. These proteins belong to different families and have a manifold of functions including enzymatic activities needed for cell wall synthesis and modification,

enzymes using (host) substrates in the surrounding environment (e.g. aspartic proteases), proteins involved in surface adhesion and biofilm formation, and others [14]. Interestingly, genomic analyses showed enrichment of some GPI protein families (e.g. Hyr/Iff adhesins) in pathogenic *Candida* spp. compared to related non-pathogenic species, suggesting a direct relationship to pathogenicity [15].

GPI-modified adhesins confer yeasts the ability to adhere onto different substrates such as host cells or abiotic surfaces (medical devices, catheters), and thus play an important role in the establishment of infections [16, 17]. In addition, the ability to form biofilms by cell-to-cell adhesion renders an infiltrate stable matrix that enhances resistance to antifungal agents [18]. GPI proteins in *C. albicans* include three adhesin families: Als [19], Hyr/Iff [20] and Hwp [21]. Genomic analyses have shown that these adhesin families are conserved in other *Candida* species of the CTG clade [15]. For the non-CTG clade pathogenic yeast *Candida glabrata* similar genomic studies demonstrated that it contains an extraordinarily large number of more than 70 sequences encoding GPI-modified adhesin-like proteins [22–26]. Recent structural studies showed that most of these adhesins can be divided into two groups: (i) Epa1-related proteins with shown or presumed host-binding lectin activities and containing N-terminal PA14-like domains similar to flocculins in *S. cerevisiae* [27, 28], and (ii) proteins with β -helix/ β -sandwich N-terminal domains for which the substrate ligands are still unidentified although involvement in adherence to polystyrene surfaces was demonstrated for Awp2 [29].

Following adhesion to host cells, *Candida* species secrete enzymes that help to disrupt host membranes and proteins and actively penetrate into tissues [30], as well as improve the efficiency of extracellular nutrient acquisition [31]. Three different classes of such secreted or cell wall hydrolases, namely aspartic proteases, phospholipases, and lipases have been described [32]. Among the aspartic proteases and phospholipases, some members may be retained into the cell wall through GPI anchoring [15, 33, 34]. Expansion of genes encoding aspartic proteases in pathogenic species compared to less pathogenic relatives supports a role for these proteins in the infection process [15, 35].

Thorough knowledge of the cell wall structure and its proteomic composition is crucial to better understand biofilm formation and host-pathogen interactions underlying *Candida* pathogenesis. However, in *P. kudriavzevii* this remains poorly studied to date. The aim of this study therefore was to enhance our knowledge of the *P. kudriavzevii* cell wall through an integrated approach including a comprehensive genomic inventory of its cell wall biosynthetic machinery, analysis of its cell wall composition and proteome, and surface adhesion and biofilm formation studies. Intriguingly, proteomic analysis of flor formed during static culturing revealed increased expression of a Flo11-like wall protein potentially important for biofilm formation during infection.

Results

The cell wall synthetic genetic machinery of *P. kudriavzevii*

Here, we present a multidisciplinary study to enhance our knowledge about synthesis and composition of the cell wall in the human pathogenic yeast *P. kudriavzevii*. First, an extensive bioinformatic analysis of its cell wall biosynthetic genetic machinery was carried out on the translated genome of reference strain CBS573 using known fungal cell wall biosynthetic genes as search queries. BLAST queries comprised any experimentally validated fungal cell wall gene known to us, however, identified genes were limited to homologs picked up with *C. albicans* and *S. cerevisiae* queries. Cell walls of CTG-clade *Candida* species and *S. cerevisiae* are mainly composed of a network of the polysaccharides, β -1,3-glucan, β -1,6-glucan, and chitin, to which a variety of glycoproteins are covalently attached either to β -1,6-glucan through GPI

remnants, or to β -1,3-glucan through mild-alkali sensitive linkages (ASL). Synthesis of β -1,3-glucan and chitin is carried out by enzyme complexes located in the plasma membrane. The corresponding genes, as well as those of proteins involved in synthesis of precursor molecules or with regulatory functions, for instance the cell wall integrity pathway, appear mostly conserved in *P. kudriavzevii* with similar representation in the genome as described for *C. albicans* and *S. cerevisiae* (Tables 1; details in S1) [15]. However, the genomic analysis of *P. kudriavzevii* revealed reductions in the numbers of genes in glycosyl hydrolase families GH5 (Exg), GH81 (Eng), and GH18 (Cht), implicated in modification or hydrolysis of β -1,3-glucan and chitin, for instance during cytokinesis.

Synthesis of cell wall β -1,6-glucan in yeasts is a poorly understood process although the molecule has a crucial role in interconnecting β -1,3-glucan, chitin, and GPI-modified mannoproteins. For instance, a β -1,6-glucan-synthetizing enzyme remains unidentified to date even though Kre6-like GH16 proteins have been postulated as candidates [36, 37]. Noteworthy, where *C. albicans* contains four and *S. cerevisiae* two Kre6-like paralogs, Kre6 and its twin paralog Skn1 that arose from the whole genome duplication, *P. kudriavzevii* contains only a single Kre6 homolog in its genome.

The Dfg5 GH76 family of putative endo-mannanases is described to hydrolyze glycan moieties of GPI anchors for subsequent attachment of GPI proteins to non-reducing ends of β -1,6-glucan in the cell wall [38–40]. Most *Candida* species and *S. cerevisiae* contain two *DFG5*-related genes, but three paralogs are present in *P. kudriavzevii* (Table 1). In contrast, for the Ecm33 family, proposed to have a—still unresolved—role in CWP or β -1,6-glucan incorporation [41, 42], only two genes are present in *P. kudriavzevii* whereas *C. albicans* contains three and *S. cerevisiae* four (two twin pairs) paralogs.

Proteins that are destined to be covalently bound to the cell wall polysaccharide network are secretory proteins. After synthesis of their precursors, they are translocated to the cell surface and usually become highly glycosylated during their passage through the endoplasmic reticulum and Golgi apparatus. Glycosylation in *Candida* occurs via two different processes, O- and N-glycosylation. O-glycans are short mannan chains of up to five residues connected to hydroxyl side chains of serine (Ser) and threonine (Thr) residues. As CWPs usually have a high percentage of these residues, O-glycosylation contributes significantly to the mannan present in the cell wall of *Candida*. N-glycosylation occurs less frequently, as its acceptor molecules are side chain nitrogen atoms of asparagine (Asn) residues that are part of an Asn–X–Ser/Thr consensus sequence (where X is any amino acid except proline). However, individual N-glycan chains may contain up to 200 mannose residues, added by diverse families of mannosyltransferases, and thus also greatly contribute to the cell wall mannan content. Interestingly, in *P. kudriavzevii* clear differences are observed in the gene copy repertoire of mannosyltransferases compared to *C. albicans*. While *C. albicans* contains two Och1-like GT32 α -1,6-mannosyltransferases needed for N-glycan outer chain backbone formation, *P. kudriavzevii* contains five Och1 paralogs. Further, the GT15 (*Pk* 11 versus *Ca* 5 genes) and GT71 (*Pk* 12 versus *Ca* 6 genes) families of presumed α -1,2-mannosyltransferases are also largely extended in *P. kudriavzevii*. On the other hand, the analyzed genome of *P. kudriavzevii* contains only one GT91 β -1,2-mannosyltransferase gene, whereas this family consists of nine paralogs in *C. albicans*, and the number of Mnn4-like regulators of mannosylphosphorylation of N-linked mannans is also reduced (*Pk* 3 versus *Ca* 9 genes). The Pmt family of protein-O-mannosyltransferases (GT39) comprises five paralogs in both species.

We also identified putative GPI proteins and CWPs covalently bound through mild-alkali sensitive linkages (ASL). Our bioinformatic pipeline selected 43 putative GPI protein candidates (S2 Table), which is less than described for pathogenic CTG-clade *Candida* spp. [15, 20, 43], *C. glabrata* (about 100) [44], and *S. cerevisiae* (about 70) [43] using similar approaches.

Table 1. Comparative analysis of protein families involved in cell wall biosynthesis of *P. kudriavzevii*.

Protein class ¹	<i>Pk</i> ²	<i>Ca</i>	<i>Sc</i>
<i>β-1,3-glucan synthesis and processing</i>			
Fks family. β -1,3-glucan synthases (GT48)	3	3	3
Rho-related GTPases regulating β -1,3-glucan synthesis; Rho1-like	6	6	6
Regulators of cell wall synthesis; Smi1-like	2	2	1
Gas family. β -1,3-Glucanosyltransglycosylases (GH72)	5	5	5
Crh family. Transglycosylases involved in glucan-chitin crosslinking (GH16)	2	3	3
Bgl2 family. Putative β -1,3-transglucosylases (GH17)	4	5	4
Putative endo- β -1,3-glucanases (GH81); Eng1-like	1	2	2
Putative exo- β -1,3-glucanases (GH5); Exg1-like	2	3	3
Sun family. Putative β -glucosidases involved in septation (GH132)	2	2	4
<i>Chitin synthesis and processing</i>			
Chitin synthases (GT2); Chs1-like	4	4	3
Chitinases (GH18); Cts1- or Cts2-like	2	4	2
Chitin deacetylases (CE4), involved in chitosan synthesis; Cda2-like	1	1	2
<i>Protein mannosylation</i>			
Pmt family. Protein- <i>O</i> -mannosyltransferases (GT39)	5	5	7
α -1,6-Mannosyltransferases (GT32). Initiation of N-glycan outer chain branch addition; Och1-like	5	2	2
Anp1-like subunits of a Golgi α -1,6-mannosyltransferase complex (GT62)	3	3	3
Mnn10-like subunits of a Golgi α -1,6-mannosyltransferase complex (GT34)	2	2	2
Mnn4-like regulators of mannosylphosphorylation of N-linked mannans	3	8	2
Bmt family. β -1,2-mannosyltransferase (GT91). β -mannosylation of phosphopeptidomannan	1	9	0
Ktr/Mnt family of α -1,2-mannosyltransferases (GT15)	11	5	9
Mnn2 family of α -1,2-mannosyltransferases (GT71)	12	6	2
Mnn1 family of α -1,3-Mannosyltransferases (GT71)	4	6	4
<i>Other proteins with putative functions in CW synthesis</i>			
Kre6-like putative transglycosylases (GH16) required for β -1,6-glucan biosynthesis	1	4	2
Dfg5 family. Putative endo-mannanases (GH76-family) with a possible role in GPI-CWP incorporation	3	2	2
Ecm33 family. Possible role in CWP incorporation (GH NC)	2	3	4
Pir family. Putative role in β -1,3-glucan crosslinking	5	2	5

¹Classification of carbohydrate-active enzymes according to CAZy Database (<http://www.cazy.org/>).

²*Pk*, *P. kudriavzevii*; *Ca*, *C. albicans*; *Sc*, *S. cerevisiae*.

<https://doi.org/10.1371/journal.ppat.1011158.t001>

Nonetheless, the list of predicted *P. kudriavzevii* GPI proteins includes most of the protein families also described in the abovementioned species, for example, Gas, Crh, Ecm33, Dfg5, adhesins/flocculins, aspartyl proteases, and phospholipases. Detailed manual inspection of protein sequences identified during mass spectrometric CWP analysis (see below) indicated that some GPI proteins were not picked up (false negatives) by our GPI protein pipeline, probably mostly due to erroneous automated annotations.

Blast searches identified ten probable aspartyl proteases in *P. kudriavzevii*, six of which are predicted to be GPI anchored. For comparison, 13 aspartyl proteases have been described in *C. albicans*, two of which are documented as GPI proteins with cell wall localization [34]. In *C. glabrata*, nine predicted GPI-modified aspartyl proteases were identified [25] but, consistent with their absence in cell wall preparations, these proteins present dibasic motifs in the region immediately upstream of the GPI attachment site, favoring plasma membrane retention [45].

Eleven ORFs showing adhesin properties and/or weak similarity to Flo1, 5, 9 and 10 and Flo11 flocculins in *S. cerevisiae* or Ywp1/Hwp1 adhesins in *C. albicans* were identified (Tables 2

Table 2. Identified adhesin/flocculin-like proteins in *P. kudriavzevii* strain CBS573.

NCBI Refseq	Proposed Name	Closest Sc or Ca Blast homolog ¹	Closest PDB homolog (RMSD (Å))	Identified in cell wall ²
XP_029321299	Flo9	Flo9	ScFlo5, 2XJP (2.2)	Yes
XP_029321005 + XP_029321006	Flo90	Flo9	ScFlo5, 2XJP (2.6)	Yes
XP_029320844	Flo91	Flo9	ScFlo5, 2XJP (2.6)	
XP_029323952	Flo92	Flo9	ScFlo5, 2XJP (2.4)	Yes
XP_029322636	Flo10	Flo9	ScFlo5, 2XJP (2.2)	Yes
XP_029322875	Flo11	Flo11	ScFlo11, 4UYR (2.3)	
XP_029321007	Flo110	no hits	ScFlo11, 4UYR (2.7)	Yes
XP_029322143	Flo111	no hits	ScFlo11, 4UYR (3.2)	Yes
XP_029319891	Alp1	Ywp1	CaAls3, 4LEE (4.5)	
XP_029319890	Alp2	Ywp1	CaAls3, 4LEE (4.6)	
XP_029323142	Alp3	Ywp1	CaAls3, 4LEE (6.8)	

¹Sc, *S. cerevisiae*; Ca, *C. albicans*.

² See Fig 5 and S4 Table for the mass spectrometric analysis of purified cell walls.

<https://doi.org/10.1371/journal.ppat.1011158.t002>

and S1). Despite the low level or even absence of sequence similarity, their identifications as putative flocculins and adhesins was supported by tertiary (3D) structure modeling and subsequent structure-similarity analysis (Fig 1). Remarkably, (part of) the tertiary structures of the three ORFs with weak amino acid sequence similarity to Ywp1 showed more resemblance, albeit with relatively high Root Mean Square Deviation (RMSD) values, to β -sandwich structures encountered in Als3 (Figs 1 and S1). We tentatively designated these proteins adhesin-like proteins 1–3 (Alp1–3; Table 2). Manual inspection of the flocculin ORF sequences revealed that the majority seems to have incorrect ORF boundaries (S1 Table), providing a likely explanation why half of the flocculins were not identified by the GPI prediction pipeline but probably are genuine GPI proteins, in accordance with their presence in cell wall preparations (Tables 2 and S4).

Known ASL wall proteins in baker's yeast and *Candida* spp. are Pir proteins, Bgl2 and Sun4 family proteins (described above), and Tos1. Homologs of these proteins were also identified in *P. kudriavzevii* (Tables 1, S1 and S3). The Pir protein family has a proposed role in cell wall reinforcement through β -1,3-glucan crosslinking. The PIR family in *P. kudriavzevii* and *S. cerevisiae* is expanded compared to *C. albicans* (*Pk* and *Sc* 5 versus *Ca* 2 genes).

The cell wall composition of *P. kudriavzevii*

To establish relationships between the biosynthetic machinery as deduced from genomic studies and the abundance of cell wall macromolecules in *P. kudriavzevii*, we determined the cell wall composition of cells at exponential phase ($OD_{600} = 1.8$) and from floating biofilm formed after a 24 h incubation under static conditions, both in YPD at 37°C. First, the amount of glucan and mannan was determined by HPLC analysis after acid hydrolysis of purified walls from exponentially growing cells and biofilms (Table 3). In both conditions *P. kudriavzevii* contained about 50% glucan (determined as glucose), which seems slightly less than the 61.5% in *C. albicans*. In contrast, a significantly higher amount of mannan is present in walls of *P. kudriavzevii* (*Pk*: 40% versus *Ca*: 16%), consistent with differences in gene copy numbers of mannosyltransferase protein families discovered in the genomic analysis. In a complementary approach using cells grown to exponential phase ($OD_{600} = 1.8$), α -mannan was determined by binding to ConA and phosphomannan by Alcian blue binding using flow cytometry (FC).

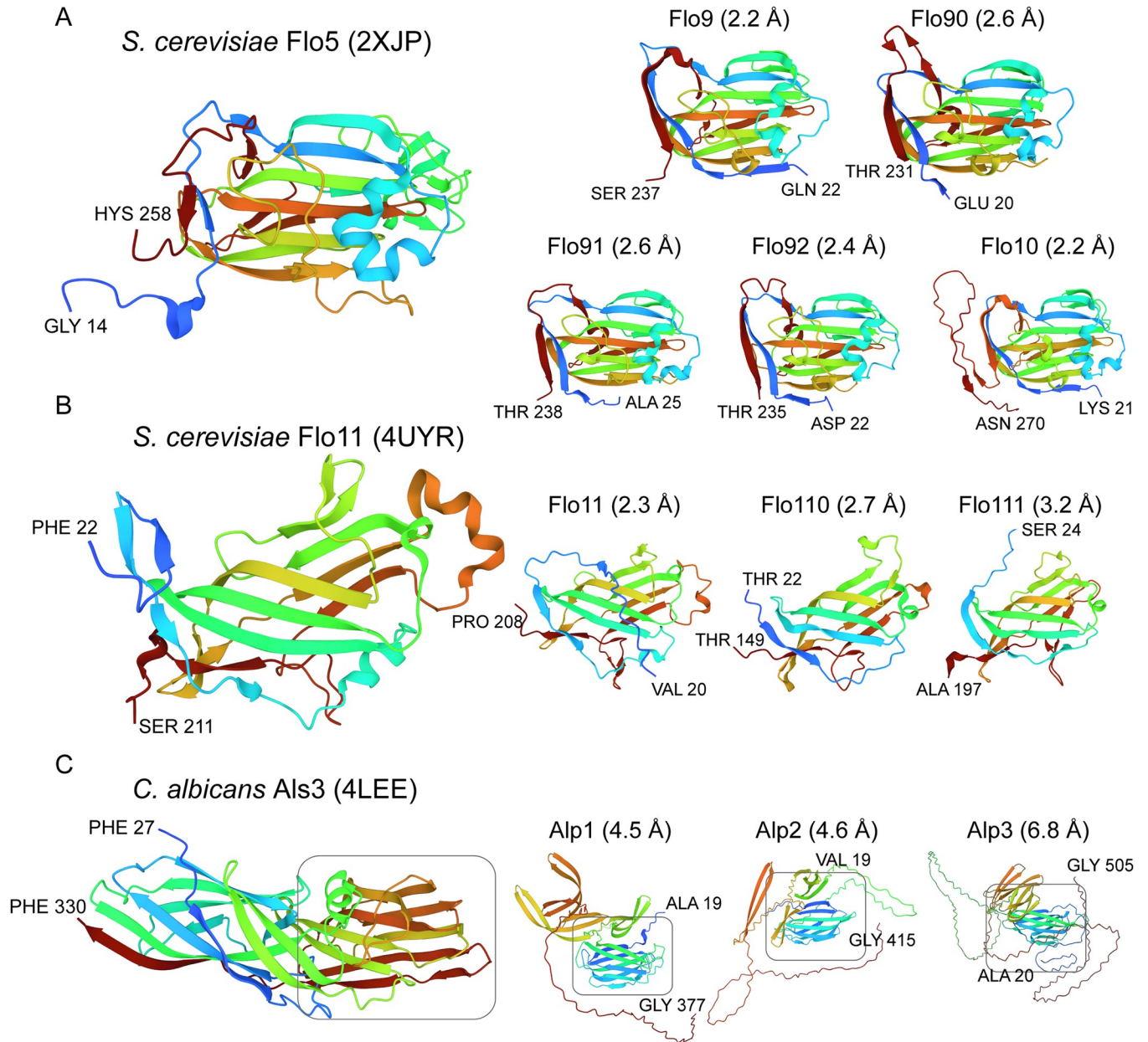


Fig 1. Tertiary (3D) structure analysis of *P. kudriavzevii* adhesins by AlphaFold modeling of putative ligand-binding domains. Predicted domain structures are shown in rainbow-color representation from blue (N-terminus) to red (C-terminus) with the first and last amino acids indicated. *P. kudriavzevii* ORFs with similarity to (A) *S. cerevisiae* flocculins Flo1,5,9 and 10 (five ORFs), (B) *S. cerevisiae* flocculin Flo11 (three ORFs), or (C) containing a β -sandwich similar to the structure present in *C. albicans* adhesin Als3 (three ORFs).

<https://doi.org/10.1371/journal.ppat.1011158.g001>

Consistent with the HPLC and genomic data, this analysis showed elevated levels of ConA binding in *P. kudriavzevii* compared to *C. albicans* (Fig 2A), also leading to increased cell aggregation in *P. kudriavzevii* but not in *C. albicans* (Fig 2C). In contrast, reduced Alcian blue binding was observed (Fig 2A), consistent with the reduced gene copy number of β -mannosyl-transferases in the genome of *P. kudriavzevii*.

Protein and chitin levels in purified cell walls were determined using colorimetric assays upon alkali and acid hydrolysis, respectively, and further explored using FC of CFW and

Table 3. *P. kudriavzevii* cell wall composition analysis and comparison to *C. albicans* and *S. cerevisiae*.

Wall Component	<i>P. kudriavzevii</i>		<i>C. albicans</i>	<i>S. cerevisiae</i>
	Exponential phase ²	Biofilm	Exponential phase	
Glucan (% dww ¹)	53.4 ± 8.2	51.2 ± 3.6 (*)	61.5 ± 7.0	55–65 ³
Manan (% dww)	39.3 ± 6.3 (*)	40.3 ± 3.5 (*)	15.8 ± 3.1	30–35 ³
Protein (% dww)	6.7 ± 0.1 (*)	10.6 ± 0.1 (*)	3.0 ± 0.1	3–5 ⁴
Chitin (% dww)	1.6 ± 0.2 (*)	1.8 ± 0.2 (*)	4.4 ± 0.2	1–2 ³

¹dww, dry weight walls. Values are means ± standard deviations. Statistically significant differences ($p < 0.05$) between *P. kudriavzevii* and *C. albicans* as indicated by Student's t-tests are marked by asterisks.

²Cultures were performed in YPD at 37°C and harvested either at OD₆₀₀ = 1.8 (exponential phase) or after a 24 h incubation under static conditions (biofilm).

^{3,4}Data from ³Yin et al. [47] and ⁴Klis et al. [48].

<https://doi.org/10.1371/journal.ppat.1011158.t003>

WGA-FITC binding to exponentially growing cells (OD₆₀₀ = 1.8). Walls from exponentially growing *P. kudriavzevii* cells contained 6.7% protein, about twofold higher than the amount in *C. albicans* (Table 3). This further increased to 10.6% in biofilm cell walls (Table 3). The determined amount of chitin present in the cell wall of *P. kudriavzevii* was lower than in *C. albicans* ($Pk/Ca = 0.37$) but similar to *S. cerevisiae*, and this was supported by CFW binding (Fig 2B). On the other hand, while WGA-FITC binding was also similar as in *S. cerevisiae*, it was about fivefold lower in *C. albicans* (Fig 2B), which seems to indicate that chitin is less exposed on the cell surface of *C. albicans* compared to *P. kudriavzevii* and *S. cerevisiae* [46].

The above-described differences in cell wall composition between *P. kudriavzevii* and *C. albicans* may affect cell surface properties. Indeed, when analyzing sensitivity to cell wall-perturbing compounds, *P. kudriavzevii* shows reduced sensitivity to zymolyase and Congo red (CR) compared to *C. albicans*, while its sensitivity to CFW is increased (Fig 3A and 3B). Also noteworthy is the different colony color between the two species upon CR staining, which might further point to an interesting difference in cell wall organization, possibly related to amyloid formation [49].

Floating biofilm formation and adhesion

We then performed experiments to evaluate *P. kudriavzevii* biofilm formation and adherence. First, biofilm formation onto polystyrene during 24 h of incubation in YPD and RPMI without shaking was analyzed. In *C. albicans* this led to cell sedimentation and subsequent biofilm formation onto the plastic in both media but for *P. kudriavzevii* this was only the case in RPMI. Interestingly, in YPD, *P. kudriavzevii* did not sediment but in contrast formed a film of floating cells, adhered to each other, at the air-liquid interface (Fig 4A). Nevertheless, adhesion of *P. kudriavzevii* to polystyrene at the air-liquid interface equaled the biofilm mass of *C. albicans* formed as a layer at the bottom in static cultures (Fig 4D). Aeration by agitation (200 rpm) in YPD led to the formation of *P. kudriavzevii* flocs that, compared to *C. albicans*, showed higher adhesion to polystyrene, probably because agitation diminishes biofilm formation of the latter (Fig 4D). Consistent with the observed flocculation (Fig 4B), growth (OD₆₀₀) measurements of liquid cultures showed that *P. kudriavzevii* reached a lower maximum cell density (Fig 4B).

Adhesion tests in PBS after 4 h of incubation (without shaking) showed that adhesion to polystyrene was also higher in *P. kudriavzevii* than in *C. albicans* (Fig 4C). We then tested whether binding to cell wall components may play a role in the observed cell-cell interactions (Fig 4C). However, binding experiments to immobilized molecules that form the internal polysaccharide layer of the cell wall, pustulan (β-1,6-glucan), laminarin (β-1,3-glucan), and chitin, showed less adhesion of *P. kudriavzevii* to these molecules compared to *C. albicans* (Fig 4C).

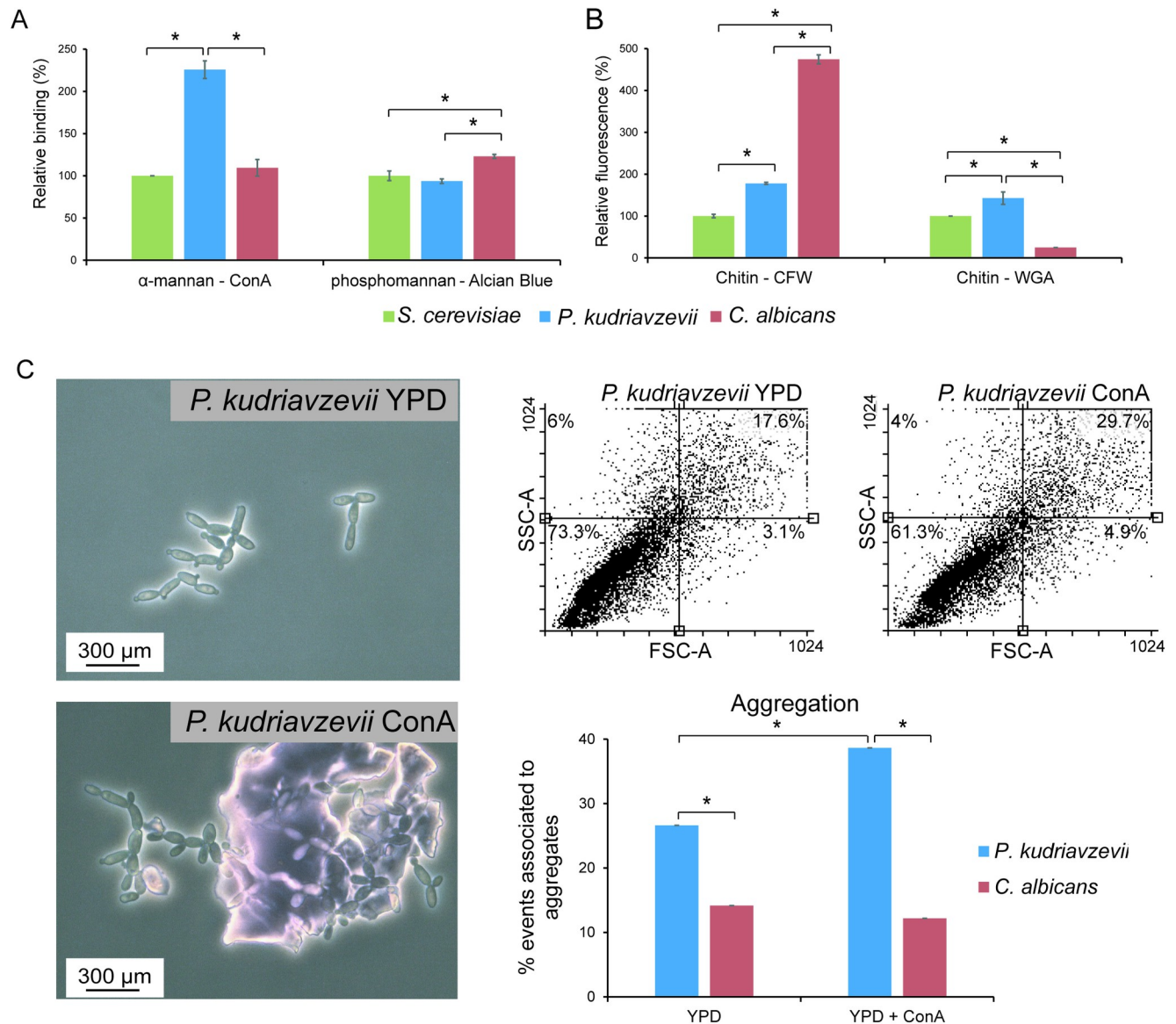


Fig 2. *P. kudriavzevii* cell wall composition and aggregation analysis. (A and B) Flow cytometry (FC) and colorimetric analysis of (A) Concanavalin A (ConA) α -mannan binding and Alcian blue phosphomannan binding and (B) Calcofluor white (CFW) and Wheat germ agglutinin (WGA) chitin binding. (C) Aggregation. Events associated to aggregates were quantified by flow cytometry, measuring 10,000 cell particles per strain in the presence or absence of Concanavalin A (ConA), FSC-A, particle size; SSC-A, particle complexity. Percentage of cell particles in each quadrant is indicated. Cell aggregation data was supported by optical microscopy. Cells used in these experiments were grown to exponential phase ($OD_{600} = 1.8$). *C. albicans* (A, B, and C) and *S. cerevisiae* (A and B) are added for comparative reasons. Data in (A) and (B) are normalized against *S. cerevisiae*. Statistically significant differences ($p < 0.05$), indicated by ANOVA and post hoc LSD test analysis, are marked by asterisks. Error bars indicate standard deviations.

<https://doi.org/10.1371/journal.ppat.1011158.g002>

In contrast, a significant increase was observed in binding of *P. kudriavzevii* to mannan and mannose (Fig 4C). With regard to host surface molecules, adhesion of *P. kudriavzevii* to collagen and galactose was lower than in *C. albicans* (Fig 4C).

Because of the high binding of *P. kudriavzevii* to mannan and mannose, we tested their influence on biofilm formation onto polystyrene in YPD (static and shaken) and RPMI (static conditions). In YPD, addition of mannan led to decreased floating biofilm formation, while in RPMI formation of biofilm onto polystyrene was not affected (Fig 4D). In contrast, *C. albicans*

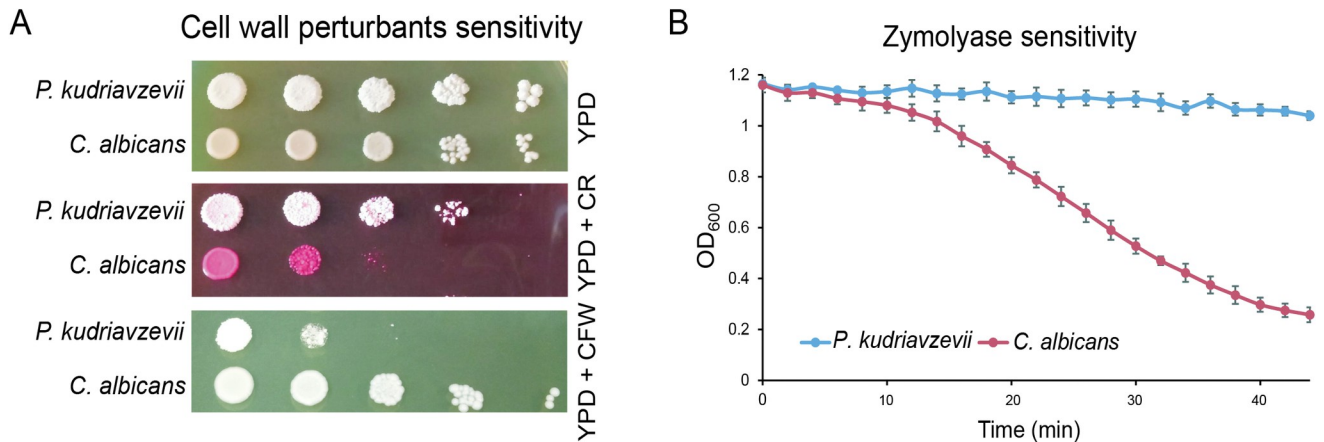


Fig 3. Cell surface properties of *P. kudriavzevii* compared to *C. albicans*. (A) Spot assays to determine sensitivity to cell wall-perturbing agents Congo red (CR; 100 $\mu\text{g}/\text{mL}$) and Calcofluor white (CFW; 100 $\mu\text{g}/\text{mL}$). (B) Zymolyase sensitivity of cells grown to early exponential phase ($\text{OD}_{600} = 1$). Error bars indicate standard deviations.

<https://doi.org/10.1371/journal.ppat.1011158.g003>

biofilm formation was increased by the addition of mannan in both media. Also noteworthy is that *C. albicans* biofilm formation in RPMI is stronger than in YPD, but this was not the case for *P. kudriavzevii*. Different than mannan, adding mannose did not affect biofilm formation in both species. Under shaking conditions in YPD, no effect of adding mannan or mannose on biofilm formation was observed (Fig 4D).

Proteomic analysis of *P. kudriavzevii* flor reveals increased incorporation of adhesins and hydrolytic enzymes

Cell aggregation in *S. cerevisiae* has been shown to be related to the expression of cell wall proteins that act as flocculins [50]. Our genomic studies revealed the presence of a similar family of flocculins in *P. kudriavzevii*. This prompted us to perform a detailed investigation of the cell wall proteome in *P. kudriavzevii*.

Proteomic analysis of cell walls from exponentially growing cultures and 24-h floating biofilms identified a total of 33 genuine CWPs whose precursors either contain signal peptides for secretion or have homology to known CWPs in other species (Fig 5A and S4 Table). All proteins except one were identified in both conditions, the remaining one, Flo10, was identified only in floating biofilms (Fig 5A and S4 Table). Consistent with our previous analyses in other *Candida* spp, the identified proteins can roughly be divided into two groups: (i) core wall proteins with similar abundance in both conditions, and (ii) condition-dependent proteins, mostly adhesins, upregulated during biofilm formation [44, 47, 51–53]. The identified core wall proteome includes carbohydrate-active enzymes from Crh, Gas, and Bgl2/Scw4 families involved in cell wall polysaccharide remodeling, non-enzymatic Pir and Srp1/Tip1 proteins with proposed roles in crosslinking of β -glucan chains, and proteins with unknown functions including Ssr1 and the widely distributed Ecm33 (Fig 5A).

Volcano plot analysis of the proteomic data by peptide counting after normalizing the spectral counts of the core proteome in both conditions (S5 Table), showed elevated incorporation of the adhesin Flo90 as well as the aspartyl protease Sap9, and phospholipase Plb1 in flor biofilms (Fig 5B). Although only Flo90 reached a statistically significant twofold change, four of the six identified putative flocculins appear to have increased abundance in biofilms. Flo9 is abundantly present in flor cells (210 peptides identified) but did not reach a twofold increase, Flo10 was identified only in biofilm (5 peptides). Flo110, was also very abundant in biofilms

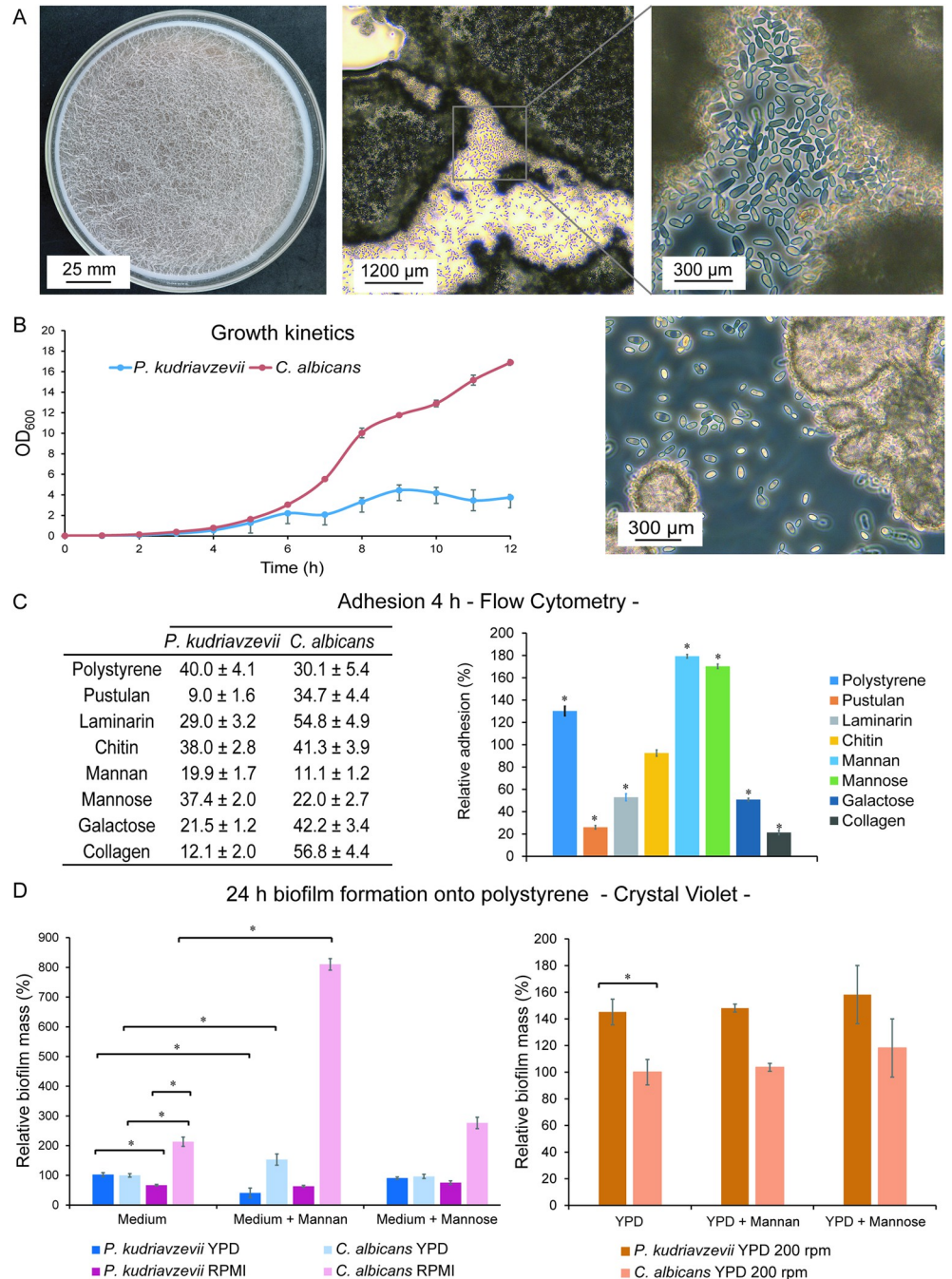


Fig 4. Adhesion and biofilm-forming properties of *P. kudriavzevii*. (A) *P. kudriavzevii* floating biofilm formation after 24 h static incubation in YPD at 37°C. Left, Petri dish showing floating biofilm; Middle and right, light microscopy images. (B) Growth kinetics. Right-hand side, representative image (light microscopy) of floc formation of *P. kudriavzevii* after 12 h. (C) Percentage of cells adhering to polystyrene and different cell wall and host surface molecules after 4 h of incubation measured by flow cytometry. In the histogram, *P. kudriavzevii* data are normalized to *C. albicans* under the same condition. (D) Biofilm biomass after 24 h measured by Crystal Violet staining. In both histograms (left, non-shaking conditions; right, shaking), data are normalized against *C. albicans* in YPD without adding mannan or mannose. Statistically significant differences ($p < 0.05$), as analyzed by Student's t-tests or ANOVA followed by post hoc LSD test analysis, are indicated by asterisks. Error bars and \pm indicate standard deviations.

<https://doi.org/10.1371/journal.ppat.1011158.g004>

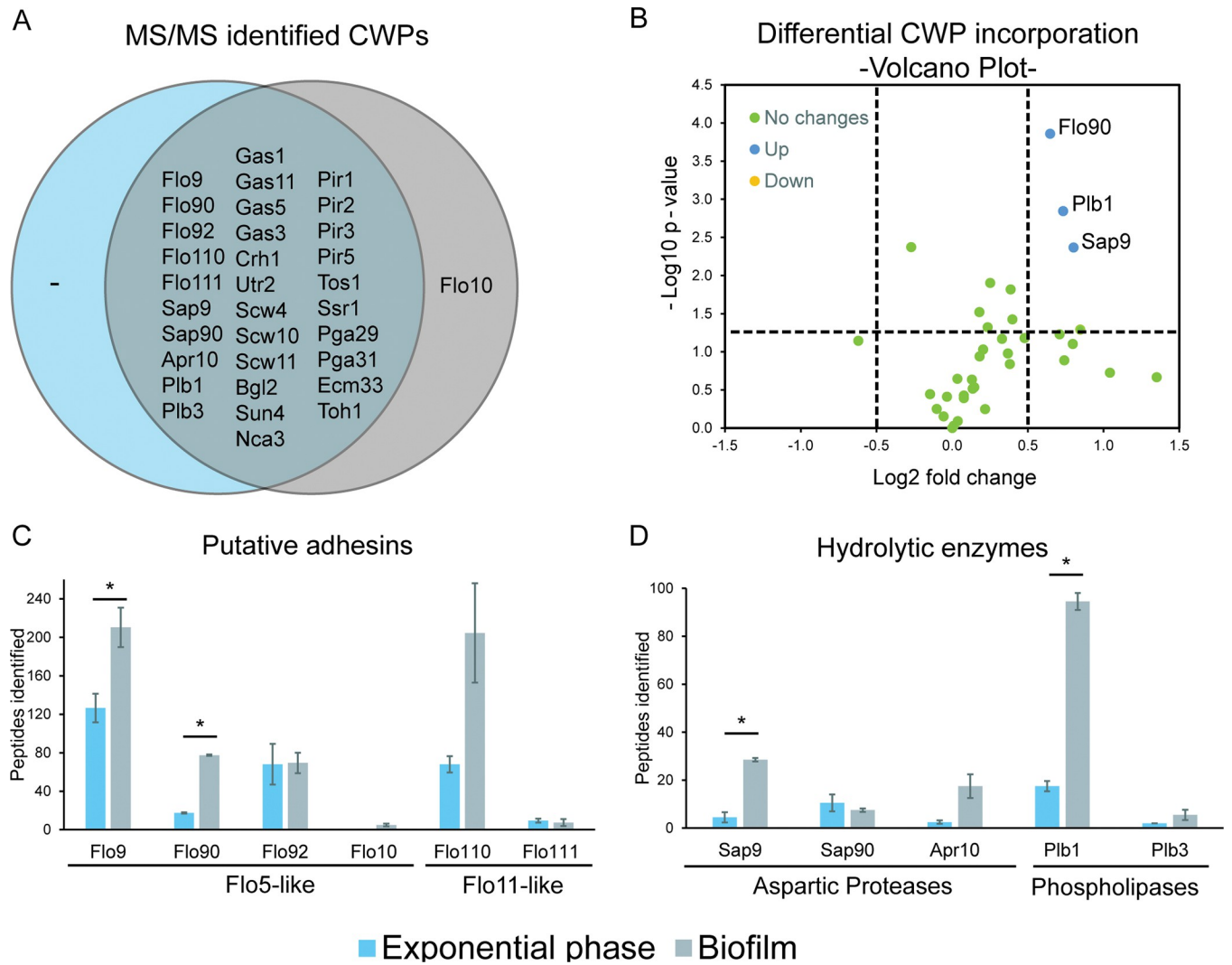


Fig 5. Comparative proteomic analysis of *P. kudriavzevii* cell walls. (A) Venn diagram showing comparative analysis of exponential phase cells and biofilms. (B) Volcano plot analysis of individual protein abundance in biofilms versus exponential phase cells. Indicated are proteins with at least twofold and statistically significant changes in abundance. (C and D) Peptide counts of putative adhesins and hydrolytic enzymes, respectively. Statistically significant differences ($p < 0.05$) between the two conditions as indicated by Student's t-tests are marked by asterisks.

<https://doi.org/10.1371/journal.ppat.1011158.g005>

(205 peptides) and reached a threefold change but lacked statistical significance due to variation between the biological duplicates (Fig 5C and S4 Table). Inferred from its similarity to *S. cerevisiae* Flo11, this protein probably plays an important role in the observed flor formation of *P. kudriavzevii*.

With respect to the hydrolytic enzymes found in the cell wall of *P. kudriavzevii*, the abundance of aspartyl proteases tripled (18 versus 54 peptides) in floating biofilm, while phospholipases almost sextupled (20 versus 112 peptides) (Fig 5D and S4 Table). Besides the already mentioned Sap9 and Plb1, abundance in biofilms also appeared increased for Apr10 (protease) and Plb3 (phospholipase), however, in both cases, without reaching statistical significance. This is the first time that such a significant increase of these hydrolytic enzymes has been observed in yeast cell walls during biofilm formation, which perhaps might be related to the special characteristics of the floating biofilm produced by this yeast.

Discussion

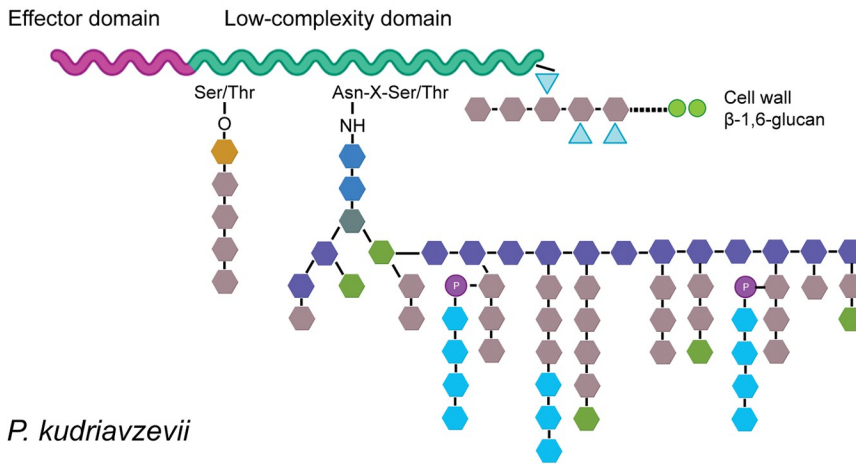
The yeast *Pichia kudriavzevii* is among the five most frequent etiological agents of candidiasis but is phylogenetically very distinct to *C. albicans* and other clinically relevant *Candida* species. Perhaps for this reason, *P. kudriavzevii* is relatively understudied [4]. This is also the case for its cell wall composition even though it is well known that the yeast cell wall plays an important role in the primary host-pathogen interactions that underlie the establishment of infections.

Here, we shed light on the cell wall composition of *P. kudriavzevii* through an integrative study including bioinformatic, biochemical, microscopic, and proteomic studies. First, through detailed *in silico* analysis the genetic machinery available to synthesize the cell wall of *P. kudriavzevii* is presented. Although our analysis included search queries for enzymes synthesizing cell wall components that have not been described in ascomycetous budding yeasts, such as α -glucan and cellulose [54], only protein families also described for *C. albicans* and/or *S. cerevisiae* yielded positive results, indicating that the composition and general architecture of the cell wall in *P. kudriavzevii* is similar to these yeasts. In this respect, our data corroborate the data presented by Navarro-Arias and colleagues [55] who documented the presence of β -1,3-glucan, chitin, *N*- and *O*-linked mannan and phosphomannan in *P. kudriavzevii*. Our bioinformatic analysis revealed that the biosynthetic glucan and chitin gene repertoire is very similar as in *C. albicans*, from which one could hypothesize that roughly similar amounts of these polysaccharides could be expected in the cell wall of *P. kudriavzevii*. The biochemical analyses mostly support this notion, however, two independent approaches, canonical acid hydrolysis with hot 6 N HCl followed by a colorimetric assay and CFW staining indicate that the level of cell wall chitin is about twofold lower in *P. kudriavzevii* than in *C. albicans*. The latter contrasts with Navarro-Arias et al. who documented elevated levels of chitin in *P. kudriavzevii* [55]. However, their data are relative (and not absolute) values produced by combined HPLC measurements of glucan, mannan, and chitin monomers in cell wall hydrolysates and assumed to account for 100% of the cell wall weight, obviously not a correct assumption. Interestingly, in contrast to CFW, our WGA-FITC binding assays showed increased staining of *P. kudriavzevii* compared to *C. albicans*, which was also observed by Navarro-Arias et al. [55]. The difference between the CFW and WGA results may be explained by differential binding specificities of these molecules for different types of chitin molecules [56], a more difficult access of the larger molecule WGA to chitin buried in internal layers of lateral walls [57], or to the fact that CFW not only binds chitin but also has some affinity for linear β -1,3-glucan [58].

In contrast to synthesis of glucan and chitin, differences in gene numbers for families related to degradation or modification of these polymers were observed between the genomes of *C. albicans* and *P. kudriavzevii*. Lowered numbers of glucanases and chitinases whose orthologs in other species are involved in cytokinesis [59] does not directly imply that cell division is occurring less in *P. kudriavzevii* as cell clumping is infrequent under unlimited growth conditions. However, it is noteworthy that, even under standard laboratory conditions, *P. kudriavzevii* cultures tend to show a high percentage of cells that are more elongated (Figs 2 and 4) and can easily be distinguished from cultures with typical oval-shaped *C. albicans* cells.

Strikingly, large differences in some of the gene families responsible for protein mannosylation during secretion were observed between *P. kudriavzevii* and *C. albicans*, suggesting major differences in glycosylation structures, especially of *N*-glycans, between the two species. More specifically, the extended family of GT32 α -1,6-mannosyltransferases in *P. kudriavzevii* suggests it may have longer *N*-glycan α -1,6-mannan outer chain backbones. These backbones may be (more) heavily decorated with short α -1,2-linked branches because of the expansion of GT15 and GT71 α -1,2-mannosyltransferases, which might also result in longer *O*-glycans. On the other hand, reduced Mnn4 (GT34) and Bmt (GT91) gene families suggests a lower level of

A. *C. albicans*



B. *P. kudriavzevii*

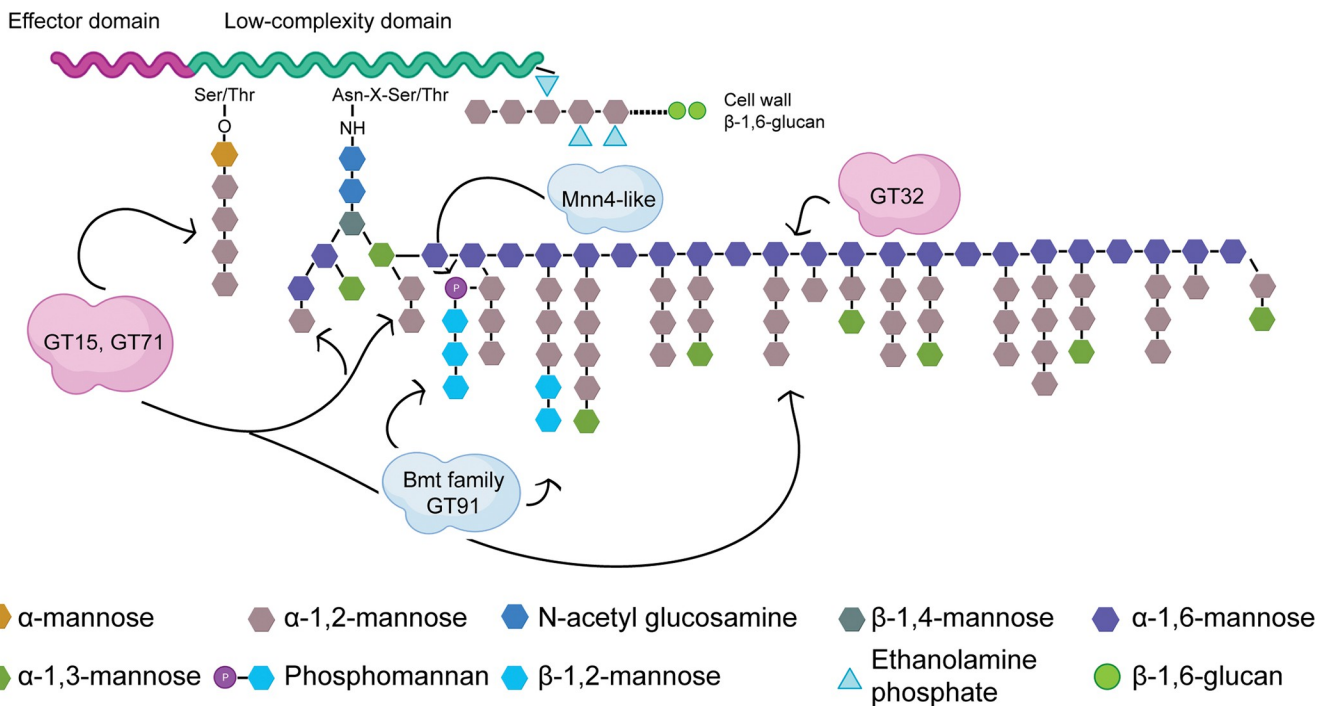


Fig 6. Schematic model showing cell wall protein mannosylation. (A) *C. albicans* protein mannosylation as described [60]. (B) Protein mannosylation in *P. kudriavzevii* as proposed in this study. Indicated in clouds are protein families expanded (pink) or reduced (grey) compared to *C. albicans*.

<https://doi.org/10.1371/journal.ppat.1011158.g006>

phosphomannan with fewer additions of β -1,2-linked mannosides to the branches (Fig 6). Our biochemical analyses are consistent with these genomic data; while the mannan content in *P. kudriavzevii* is 2.5-fold higher than in *C. albicans*, a reduction in phosphomannan was detected. Of course, we need to keep in mind that the mannan level will be related to the cell wall protein content, which is also twofold higher in *P. kudriavzevii* than in *C. albicans*. Interestingly though, where the protein content was further increased in biofilm cells, this was not or hardly the case for the mannan level.

Evaluation of biofilm formation and adherence in *P. kudriavzevii* led to the formation of floating biofilms and flocs, phenotypes that in *S. cerevisiae* are associated with the expression of flocculins in the cell wall [28]. The flocculin (Flo) family of *S. cerevisiae* includes homologous Flo1, Flo5, Flo9 and Flo10 lectins that promote cell-cell adhesion by binding to mannose, which may lead to floc formation. Interestingly, their N-terminal domains, so-called PA14 domains, show structural similarity to those in Epa proteins of the pathogen *C. glabrata*, which have been shown to bind oligosaccharides with terminal galactosyl residues of human glycoproteins, suggesting a direct role in host-pathogen interaction [61, 62]. On the other hand, *S. cerevisiae* also contains the apparently unrelated Flo11 that promotes cell-cell adhesion in a weaker manner, contains sequences promoting the formation of amyloids [63] (S2 Fig), and is essentially required for biofilm formation [64]. The *P. kudriavzevii* genome encodes at least eight putative flocculins, including five Flo5-like and three Flo11-like proteins. Mass spectrometric analysis of purified walls revealed the presence of six of these flocculins (four Flo5-like and two Flo11-like), four of which are upregulated in floating biofilm cells compared to the exponential growth phase, as judged by peptide counting. Presence of peptide sequences with possible roles in β -aggregation was suggested by Tango prediction for both Flo11-like proteins (S2 Fig). Interestingly, Flo110 is one of the most abundant wall proteins in *P. kudriavzevii* floating biofilm cells. Altogether, this suggests that these proteins, but especially Flo110, may play a key role in mediating formation of the floating biofilm.

As in our previous studies, including pathogenic as well as non-pathogenic yeast species [44, 47, 51–53], proteomic analysis of purified *P. kudriavzevii* cell walls yielded a subset of the predicted GPI and ASL proteins. This raises the interesting question why the remaining predicted CWPs were not identified. One important explanation is that part of the predicted GPI proteins is retained at the plasma membrane. However, the above-mentioned studies also showed that the identified wall proteome can roughly be divided in two groups: the majority are constitutive or core wall proteins whose levels are constant, but expression of a small number, often including adhesins, depends on the genetic background or growth conditions. This also seems the case for *P. kudriavzevii* where (only) some adhesins and hydrolytic enzymes showed higher abundance in biofilm than exponentially growing cells. Possibly, some other CWPs that remained undetected under the analyzed conditions are expressed under alternative conditions such as in the host.

Finally, the increased abundance in biofilm cells of hydrolytic enzymes, the aspartic proteases Sap9 and Apr10 and phospholipases Plb1 and Plb3, fits well with increased Sap9 and Plb3 levels in walls of *C. albicans* cells grown with lactate as carbon source compared to glucose-grown cells [65]. Increased Sap9 levels in *C. albicans* cell walls have also been observed under increased temperatures and fluconazole stress [66, 67], and expression of *C. albicans* SAP9 has been associated with adhesion and damage of epithelial cells [68].

In conclusion, our integrated study combining *in silico* and *in vitro* experiments provides important novel insights into the biosynthesis, composition, and architecture of the cell wall of *P. kudriavzevii*, including the identification of cell wall proteins that might play key roles in host-pathogen interactions, particularly relating to flocculins and floating biofilms. This may eventually lead to breakthroughs in the discovery of new treatments or novel management strategies for this pathogenic yeast.

Materials and Methods

In silico genomic analysis

P. kudriavzevii bioinformatic analysis was carried out with the genome sequence of reference strain CBS573, assembly ASM305444v1 [6], retrieved from NCBI (<https://www.ncbi.nlm.nih>.

gov). Homology studies were performed using a local BLAST tool downloaded from EMBOSS <http://emboss.sourceforge.net/>, for which known fungal cell-wall related protein sequences from related species, mostly *S. cerevisiae* and *C. albicans*, were used as queries (listed in S1 Table). Homologs identified by BLAST were judged by probability (E) values and identity levels over the whole sequence (in most cases >30%), and the presence of known functional domains. To further validate the hits, cross-BLAST searches with the identified genes as search queries were performed against the NCBI database. Putative GPI proteins were identified using a pipeline approach as described [69]. In brief, prediction of C-terminal GPI-modification sites was performed using two complementary approaches: (i) a selective fungal-specific algorithm named Big-PI, available at http://mendel.imp.ac.at/gpi/fungi_server.html [70], and (ii) a more inclusive pattern and composition scanning using the web tool ProFASTA, available at <http://www.bioinformatics.nl/tools/profasta/>, as detailed in [69]. Positive proteins from both approaches were filtered using ProFASTA, and further analyzed to select proteins that contain N-terminal signal peptides but lack internal transmembrane domains using SignalP and TMHMM servers at DTU (<https://services.healthtech.dtu.dk/>) with default settings, followed by ProFASTA parsing. As a last step in the pipeline, likely false positives were removed if NCBI-BLAST analysis indicated homology with intracellular proteins. Completeness of identified gene sets and correctness of ORF boundaries were verified by repeating the bioinformatic screens with translated assemblies of strains 129, Ckrusei653, and SD108 present in NCBI.

Protein structural modeling and analysis

Three-dimensional structures of putative adhesin ligand-binding domains were modeled using the AlphaFold2 algorithm available at the ColabFold server [71] and subsequently visualized using iCn3D [72]. Ligand-binding domains were defined as the N-terminal high-complexity regions of these proteins identified by manual inspection of the amino acid sequences. Structure similarity analysis against the proteins in the PDB database was performed using two free available algorithms: the DALI server [73] and PDBeFold, both with a default cut-off for lowest acceptable similarity match of 70% [74]. Structural pairwise alignment was executed with a web tool from the RCSB Protein Data Bank available at <https://www.rcsb.org/alignment>. TANGO was used for prediction of β -aggregation (<http://tango.crg.es/about.jsp>).

Cell culturing

Yeast strains used in this study are the reference strains *P. kudriavzevii* CBS573, *C. albicans* SC5314 and *S. cerevisiae* CEN.PK113-7D, the latter two for comparative purposes. Culturing was performed in liquid YPD (1% yeast extract, 2% peptone, 2% glucose) at 37°C and 200 rpm unless mentioned otherwise. For development of *P. kudriavzevii* biofilms, cells were precultured overnight in YPD at 37°C, and then adjusted to a cell density of $OD_{600} = 0.5$ in fresh YPD or Roswell Park Memorial Institute (RPMI) 1640 medium (Thermo Fisher). Twenty mL of the cell suspension was pipetted into a polystyrene Petri dish and incubated at 37°C for 24 h in a humid environment without shaking. Floating biofilm (flor) was recovered from the top of the culture with a spatula, and biofilm cells were resuspended in PBS and collected by centrifuging.

Cell wall isolation

Cell wall isolation was performed as described by De Groot et al. [51]. Briefly, cells were harvested by centrifugation and washed with cold 10 mM Tris-HCl, pH 7.5. After resuspension in 10 mM Tris-HCl, pH 7.5, the cells were disintegrated with glass beads using a FastPrep-24

instrument (MP Biomedicals) in the presence of a yeast/fungal protease inhibitor cocktail (Sigma). To remove intracellular contaminants and non-covalently associated proteins, the cell walls were washed extensively with 1 M NaCl, incubated twice for 5 min at 100°C in a buffer containing 2% SDS, 150 mM NaCl, 100 mM Na₂EDTA•2H₂O, 100 mM β-mercaptoethanol and 50 mM Tris-HCl, pH 7.8, and afterwards washed five times with water, each step followed by centrifugation (5 min at 3300 g). Purified walls were lyophilized and stored at -80°C until use.

Cell wall components content determination

For the determination of total cell wall glucan and mannan, purified cell walls were hydrolyzed with sulfuric acid [75] and the amount of glucose and mannose was determined by HPLC according as described [76]. Protein and chitin content were determined using colorimetric assays as described by Kapteyn et al. [77]. Values shown are expressed as the percentage of dry weight walls (% dww) and are the mean ± standard deviations of duplicate measurements from two independent experiments. Further, determination of the relative phosphomannan content and fluorescent staining of mannoprotein and chitin was performed with exponential phase cultures (OD₆₀₀ = 1.8). Phosphomannan was determined colorimetrically, using the Alcian Blue (Sigma) binding assay as described by Li et al. [78]. Mannoprotein was quantified by fluorescent staining with Rhodamine-ConA (Fisher Scientific, 100 μg/ mL), and chitin was stained with CFW (Glentham Life Science, 25 μg/ mL) and Wheat germ agglutinin (WGA)-FITC (Sigma, 100 μg/ mL). The fluorescence intensity was determined by flow cytometry.

Aggregation

Cell aggregation of exponential phase cultures (OD₆₀₀ = 1.8) in YPD was analyzed with a Leica DM1000 microscope mounted with a MC170 HD digital camera and by flow cytometry by measuring size (FSC-A) and granularity (SCC-A) of 10,000 cell particles. Effects on the addition of Concanavalin A (ConA) on aggregate formation were studied by incubating log phase cultures for at least 45 min at 37°C.

Congo red and Calcofluor white sensitivity spot assays

To reveal possible alterations in cell wall organization, sensitivity to the cell wall-perturbing compounds Congo red (CR) and Calcofluor white (CFW) was assayed using drop tests. Overnight precultures were diluted to an OD₆₀₀ = 1. From these, tenfold dilution series were prepared, and 4 μL aliquots were spotted on YPD plates containing different concentrations of CFW (100 μg/mL) and CR (100 μg/mL). Growth was monitored after 24 h of incubation at 37°C.

Zymolyase sensitivity assay

Cells were grown to exponential phase (OD₆₀₀ = 1), centrifuged, and resuspended in 10 mM Tris-HCl, pH 7.5 at an OD₆₀₀ = 2. Then, 2.5 μL/mL β-mercaptoethanol was added, and the cells were incubated for 1 h at room temperature. After this, 1.8 mL of the cell suspension and 200 μL of up to 100 U/mL zymolyase 20T were mixed, and decrease in OD₆₀₀ because of cell lysis was measured every two min after a short mixing over a period of 45 min.

Measurement of 4 h adhesion to polystyrene

For the analysis of the capacity to adhere (rather than form biofilms) to polystyrene, overnight precultures of strains of interest were adjusted to 10⁶ cells/mL in PBS, and polystyrene 12-wells

plates were filled with 500 μ L of the cell suspension. After a 4 h incubation at 37°C, unbound cells were removed by two washes with PBS. Adhered cells were then disentangled by enzymatic digestion using 100 μ L of a 2.5% trypsin (Sigma-Aldrich) solution and resuspended in 500 μ L PBS. The quantity of adhered cells was measured using a MacsQuant flow cytometer (Miltenyi Biotec, Madrid, España).

Adhesion to fungal cell wall components and host surface molecules

Differences in the binding capacity to cell wall components or to the mammalian extracellular matrix (ECM) molecules collagen and galactose was evaluated by flow cytometry. Twelve-wells microtiter plates were coated with pustulan (β -1,6-glucan, Calbiochem; 250 μ g/mL in 50 mM potassium acetate buffer), laminarin (β -1,3-glucan, Thermo Fisher; 250 μ g/mL in milli-Q water), chitin (Sigma; 250 μ g/mL in 1% acetic acid), mannan (mannan from *S. cerevisiae*, Sigma; 250 μ g/mL in milli-Q water), mannose (D-(+)-mannose, Sigma; 250 μ g/mL in milli-Q water), galactose (D-(+)-galactose LS, Panreac; 250 μ g/mL in milli-Q water) or bovine collagen (Sigma; 250 μ g/mL in 0.2 M bicarbonate buffer, pH 9.6) by adding 500 μ L of the respective solutions, and allowing for evaporation (overnight at 37°C), in the case of laminarin, pustulan, mannan, mannose, and galactose, or passive adsorption (1 h at 30°C followed by overnight incubation at 4°C), in the case of chitin and collagen. The plates were then washed with PBS. Overnight cultures of strains of interest were adjusted to 10⁶ cells/mL in PBS, and coated wells were filled with 500 μ L of the cell suspension. After 4 h of incubation at 37°C, unbound cells were aspirated and further removed by two washes with PBS. Adhered cells were loosened with a 2.5% trypsin solution, resuspended in 500 μ L PBS, and measured using a MacsQuant flow cytometer.

Quantitation of biofilm formation

For analysis of the biofilm formation capacity, the OD₆₀₀ of overnight precultures was adjusted to 2, and polystyrene 96-wells plates were filled with 50 μ L of the cell suspension and 150 μ L of fresh YPD or RPMI medium. For each strain and condition, at least two biological replicates, eight technical replicates each, were analyzed. After a 24 h incubation in a humid environment with or without shaking, the spent medium was removed, and the biofilms were washed once by immersion in a mQ water bath to remove unbound cells. Biofilm cells were stained with a 0.1% crystal violet (CV) (Sigma-Aldrich) solution for 30 min. Excess of CV was removed, and the cells were washed two times with mQ water. Stained adhered cells were resuspended in 33% acetic acid, and the intensity of CV staining was measured as OD₅₉₅ using a microtiter plate reader SpectraMax 340PC (Molecular Devices, CA). The effect on biofilm formation of supplementing the growth media with 250 μ g/mL of mannan or mannose was measured following the same protocol.

Growth kinetics

Cells from overnight precultures were diluted to an OD₆₀₀ = 0.1 in fresh YPD and incubated at 37°C and 200 rpm for 12 h, measuring the OD₆₀₀ every hour. Cell aggregation was determined at the end of the assay by optical microscopy.

Mass spectrometric identification of CWPs

Sample preparation. Reduction, S-alkylation, and proteolytic digestion of cell walls with Trypsin Gold (Promega, Madrid, Spain) were performed as described [47]. Released peptides were freeze-dried and taken up in 50% acetonitrile (ACN) and 2% formic acid. Samples were diluted

with a 0.1% trifluoroacetic acid (TFA) solution to reach a peptide concentration of about 250–500 fmol/ μ L. Duplicate biological samples were analyzed by LC-MS/MS using a timsTOF Pro (trapped ion mobility spectrometry coupled with quadrupole time of flight Pro) mass spectrometer (Bruker Daltonics) equipped with an Ultimate 3000 RSLC nano ultra-high-performance liquid chromatography (UHPLC system) (Thermo Scientific). Two hundred ng of a tryptic digest cleaned on a TT2 TopTips column was injected into a C18 Aurora column (IonOpticks) (25-cm length by 75- μ m inner diameter, 1.6- μ m particle size). The peptides were eluted from the column by applying a gradient, from 0.1% formic acid 3% ACN to 0.1% formic acid 85% ACN (flow rate, 400 nl/min), in 140 min. For the acquisition cycle, scans were acquired with a total cycle time of 1.16 s. MS and MS/MS spectra were recorded from 100 to 1,700 m/z. The raw proteomic data has been submitted to ProteomeXchange (accession number PXD041801) through the MassIVE partner repository.

MS/MS database searching. Raw MS/MS data were processed with Data Analysis software (Bruker, Billerica, MA, USA). Resulting.mgf data files were used for searching with licensed Mascot software (Version 2.5.1) against a non-redundant *P. kudriavzevii* protein database containing protein sequences downloaded from NCBI. Simultaneously, searches were performed against a common contaminants database (compiled by the Max Planck Institute of Biochemistry, Martinsried, Germany) to minimize false identifications. Mascot search parameters were: a fixed modification of carbamidomethylated cysteine, variable modification of oxidized methionine, deamidated asparagine or glutamine, trypsin with the allowance of one missed cleavage, peptide charge state +2, +3 and +4, and decoy database activated. Peptide and MS/MS mass error tolerances were 0.3 Da. Probability-based MASCOT scores (<http://www.matrixscience.com/>, accessed on April 2nd, 2022) were used to evaluate the protein identifications with a 1% false discovery rate as the output threshold. Peptides with scores lower than 20 were ignored. Unmatched peptides were subjected to a second Mascot search with semitrypsin as the protease setting, N/Q deamidation as extra variable modification, and a cutoff peptide ion score of 40. Semitryptic peptides identified in the second search served solely to extend the sequence coverage of proteins identified in the first trypsin search. Protein identifications based on a single peptide match were only taken into consideration if identified in multiple samples and at least one time in duplicate samples. The total number of peptides identified for each protein was determined by adding up all MS/MS fragmentation spectra, leading to protein identification in the two duplicate samples.

Protein quantitation. Relative abundance of identified individual CWPs in biofilms and exponentially growing cells was determined by their total spectral MS/MS counts after normalizing the data for the total number of cell wall peptides identified in each condition.

Statistical analysis

Each assay was performed with at least two biological and two technical replicates unless otherwise stated. Statistical analysis was performed using SPSS v21.0 (IBM). Distribution of the data was analyzed using the Shapiro-Wilk test. As our data showed normal distribution, parametric Student's t-test (if two samples), or ANOVA (if more than two samples) followed by post hoc Least Significant Difference (LSD) tests were applied. P-values of <0.05 were considered statistically significant.

Supporting information

S1 Fig. Pairwise structural alignments of Alp1-3 and (A) the N-terminal ligand-binding domain of *C. albicans* Als3 (4LEE) and (B) the predicted AlphaFold2 three-dimensional

structure of *C. albicans* Ywp1. The *C. albicans* proteins are presented in grey color.
(TIF)

S2 Fig. TANGO beta-aggregation propensities of Flo11-like proteins identified in *P. kudriavzevii* cell walls by MS/MS. *S. cerevisiae* Flo11 is added for comparison. N-terminal domains of the proteins are eliminated for clarity. Vertical arrows indicate C-terminal ends of each protein.
(TIF)

S1 Table. Proteins involved in cell wall synthesis of *Pichia kudriavzevii*.
(XLSX)

S2 Table. Putative GPI proteins identified in *Pichia kudriavzevii* using a predictive bioinformatic pipeline.
(XLSX)

S3 Table. Predicted ASL proteins in *Pichia kudriavzevii*.
(XLSX)

S4 Table. MS/MS identification of cell wall proteins in *Pichia kudriavzevii* reference strain CBS573.
(XLSX)

S5 Table. Protein quantitation by MS/MS spectral counts.
(XLSX)

Acknowledgments

We thank Henk L. Dekker (Mass Spectrometry of Biomolecules, University of Amsterdam) and Dr. Sergi Ferrer (University of Valencia) for technical support in the analysis of the cell wall protein and sugar composition, respectively.

Author Contributions

Conceptualization: María Alvarado, Emilia Gómez-Molero, Gertjan Kramer, Piet W. J. De Groot.

Data curation: Carmen Berbegal, Piet W. J. De Groot.

Formal analysis: Jesús Alberto Gómez-Navajas, María Teresa Blázquez-Muñoz, Carmen Berbegal.

Funding acquisition: Elena Eraso, Gertjan Kramer, Piet W. J. De Groot.

Investigation: María Alvarado, Jesús Alberto Gómez-Navajas, María Teresa Blázquez-Muñoz, Emilia Gómez-Molero, Carmen Berbegal, Piet W. J. De Groot.

Supervision: Emilia Gómez-Molero, Gertjan Kramer, Piet W. J. De Groot.

Writing – original draft: María Alvarado, Piet W. J. De Groot.

Writing – review & editing: María Alvarado, Elena Eraso, Gertjan Kramer, Piet W. J. De Groot.

References

1. Quindos G. Epidemiology of candidaemia and invasive candidiasis. A changing face. Rev Iberoam Micol. 2014; 31(1):42–8. <https://doi.org/10.1016/j.riam.2013.10.001> PMID: 24270071

2. McCarty TP, Pappas PG. Invasive Candidiasis. *Infect Dis Clin North Am.* 2016; 30(1):103–24. <https://doi.org/10.1016/j.idc.2015.10.013> PMID: 26739610
3. Pappas PG, Lionakis MS, Arendrup MC, Ostrosky-Zeichner L, Kullberg BJ. Invasive candidiasis. *Nat Rev Dis Primers.* 2018; 4:18026. <https://doi.org/10.1038/nrdp.2018.26> PMID: 29749387
4. Gomez-Gaviria M, Mora-Montes HM. Current Aspects in the Biology, Pathogeny, and Treatment of *Candida krusei*, a Neglected Fungal Pathogen. *Infect Drug Resist.* 2020; 13:1673–89.
5. Yadav JS, Bezawada J, Yan S, Tyagi RD, Surampalli RY. *Candida krusei*: biotechnological potentials and concerns about its safety. *Can J Microbiol.* 2012; 58(8):937–52.
6. Douglass AP, Offei B, Braun-Galleani S, Coughlan AY, Martos AAR, Ortiz-Merino RA, et al. Population genomics shows no distinction between pathogenic *Candida krusei* and environmental *Pichia kudriavzevii*: One species, four names. *PLoS Pathog.* 2018; 14(7):e1007138.
7. Borman AM, Johnson EM. Erratum for Borman and Johnson, "Name Changes for Fungi of Medical Importance, 2018 to 2019". *J Clin Microbiol.* 2021; 59(4). <https://doi.org/10.1128/JCM.00331-21> PMID: 33826524
8. Samaranyake YH, Wu PC, Samaranyake LP, Ho PL. The relative pathogenicity of *Candida krusei* and *C. albicans* in the rat oral mucosa. *J Med Microbiol.* 1998; 47(12):1047–57.
9. Costa CR, Passos XS, e Souza LK, Lucena Pde A, Fernandes Ode F, Silva Mdo R. Differences in exoenzyme production and adherence ability of *Candida* spp. isolates from catheter, blood and oral cavity. *Rev Inst Med Trop Sao Paulo.* 2010; 52(3):139–43.
10. Vargas K, Srikantha R, Holke A, Sifri T, Morris R, Joly S. *Candida albicans* switch phenotypes display differential levels of fitness. *Med Sci Monit.* 2004; 10(7):BR198–206.
11. Park SJ, Han KH, Park JY, Choi SJ, Lee KH. Influence of bacterial presence on biofilm formation of *Candida albicans*. *Yonsei Med J.* 2014; 55(2):449–58.
12. Gow NA, van de Veerdonk FL, Brown AJ, Netea MG. *Candida albicans* morphogenesis and host defence: discriminating invasion from colonization. *Nat Rev Microbiol.* 2011; 10(2):112–22.
13. Klis FM, De Groot P, Hellingwerf K. Molecular organization of the cell wall of *Candida albicans*. *Med Mycol.* 2001; 39 Suppl 1:1–8.
14. De Groot PWJ, Ram AF, Klis FM. Features and functions of covalently linked proteins in fungal cell walls. *Fungal Genet Biol.* 2005; 42(8):657–75. <https://doi.org/10.1016/j.fgb.2005.04.002> PMID: 15896991
15. Butler G, Rasmussen MD, Lin MF, Santos MAS, Sakthikumar S, Munro CA, et al. Evolution of pathogenicity and sexual reproduction in eight *Candida* genomes. *Nature.* 2009; 459(7247):657–62.
16. Sundstrom P. Adhesion in *Candida* spp. *Cell Microbiol.* 2002; 4(8):461–9.
17. Tronchin G, Pihet M, Lopes-Bezerra LM, Bouchara JP. Adherence mechanisms in human pathogenic fungi. *Med Mycol.* 2008; 46(8):749–72. <https://doi.org/10.1080/13693780802206435> PMID: 18651303
18. d'Enfert C. Biofilms and their role in the resistance of pathogenic *Candida* to antifungal agents. *Curr Drug Targets.* 2006; 7(4):465–70.
19. Hoyer LL, Green CB, Oh SH, Zhao X. Discovering the secrets of the *Candida albicans* agglutinin-like sequence (ALS) gene family—a sticky pursuit. *Med Mycol.* 2008; 46(1):1–15.
20. Richard ML, Plaine A. Comprehensive analysis of glycosylphosphatidylinositol-anchored proteins in *Candida albicans*. *Eukaryotic Cell.* 2007; 6(2):119–33.
21. Hayek P, Dib L, Yazbeck P, Beyrouthy B, Khalaf RA. Characterization of Hwp2, a *Candida albicans* putative GPI-anchored cell wall protein necessary for invasive growth. *Microbiol Res.* 2010; 165(3):250–8.
22. De Groot PWJ, Bader O, De Boer AD, Weig M, Chauhan N. Adhesins in human fungal pathogens: glue with plenty of stick. *Eukaryot Cell.* 2013; 12(4):470–81. <https://doi.org/10.1128/EC.00364-12> PMID: 23397570
23. Desai C, Mavrianos J, Chauhan N. *Candida glabrata* Pwp7p and Aed1p are required for adherence to human endothelial cells. *FEMS Yeast Res.* 2011; 11(7):595–601.
24. Marcet-Houben M, Alvarado M, Ksiezopolska E, Saus E, De Groot PWJ, Gabaldon T. Chromosome-level assemblies from diverse clades reveal limited structural and gene content variation in the genome of *Candida glabrata*. *BMC Biol.* 2022; 20(1):226.
25. Weig M, Jansch L, Gross U, De Koster CG, Klis FM, De Groot PWJ. Systematic identification in silico of covalently bound cell wall proteins and analysis of protein-polysaccharide linkages of the human pathogen *Candida glabrata*. *Microbiology (Reading).* 2004; 150(Pt 10):3129–44.
26. Xu Z, Green B, Benoit N, Schatz M, Wheelan S, Cormack B. De novo genome assembly of *Candida glabrata* reveals cell wall protein complement and structure of dispersed tandem repeat arrays. *Mol Microbiol.* 2020; 113(6):1209–24.

27. Essen LO, Vogt MS, Mosch HU. Diversity of GPI-anchored fungal adhesins. *Biol Chem*. 2020; 401(12):1389–405. <https://doi.org/10.1515/hsz-2020-0199> PMID: 33035180
28. Willaert RG, Kayacan Y, Devreese B. The Flo Adhesin Family. *Pathogens*. 2021; 10(11). <https://doi.org/10.3390/pathogens10111397> PMID: 34832553
29. Reithofer V, Fernandez-Pereira J, Alvarado M, De Groot P, Essen LO. A novel class of *Candida glabrata* cell wall proteins with beta-helix fold mediates adhesion in clinical isolates. *PLoS Pathog*. 2021; 17(12):e1009980.
30. Wachtler B, Citiulo F, Jablonowski N, Forster S, Dalle F, Schaller M, et al. *Candida albicans*-epithelial interactions: dissecting the roles of active penetration, induced endocytosis and host factors on the infection process. *PLoS One*. 2012; 7(5):e36952.
31. Naglik JR, Challacombe SJ, Hube B. *Candida albicans* secreted aspartyl proteinases in virulence and pathogenesis. *Microbiol Mol Biol Rev*. 2003; 67(3):400–28, table of contents.
32. Hube B, Stehr F, Bossenz M, Mazur A, Kretschmar M, Schafer W. Secreted lipases of *Candida albicans*: cloning, characterisation and expression analysis of a new gene family with at least ten members. *Arch Microbiol*. 2000; 174(5):362–74.
33. Niewerth M, Korting HC. Phospholipases of *Candida albicans*. *Mycoses*. 2001; 44(9–10):361–7.
34. Schild L, Heyken A, De Groot PWJ, Hiller E, Mock M, De Koster C, et al. Proteolytic cleavage of covalently linked cell wall proteins by *Candida albicans* Sap9 and Sap10. *Eukaryot Cell*. 2011; 10(1):98–109.
35. Moran GP, Coleman DC, Sullivan DJ. *Candida albicans* versus *Candida dubliniensis*: Why Is *C. albicans* More Pathogenic? *Int J Microbiol*. 2012; 2012:205921.
36. Lesage G, Bussey H. Cell wall assembly in *Saccharomyces cerevisiae*. *Microbiol Mol Biol Rev*. 2006; 70(2):317–43.
37. Ruiz-Herrera J, Elorza MV, Valentin E, Sentandreu R. Molecular organization of the cell wall of *Candida albicans* and its relation to pathogenicity. *FEMS Yeast Res*. 2006; 6(1):14–29.
38. Kitagaki H, Wu H, Shimoi H, Ito K. Two homologous genes, DCW1 (YKL046c) and DFG5, are essential for cell growth and encode glycosylphosphatidylinositol (GPI)-anchored membrane proteins required for cell wall biogenesis in *Saccharomyces cerevisiae*. *Mol Microbiol*. 2002; 46(4):1011–22.
39. Kollar R, Reinhold BB, Petrakova E, Yeh HJ, Ashwell G, Drgonova J, et al. Architecture of the yeast cell wall. Beta(1→6)-glucan interconnects mannoprotein, beta(1→3)-glucan, and chitin. *J Biol Chem*. 1997; 272(28):17762–75.
40. Spreghini E, Davis DA, Subaran R, Kim M, Mitchell AP. Roles of *Candida albicans* Dfg5p and Dcw1p cell surface proteins in growth and hypha formation. *Eukaryot Cell*. 2003; 2(4):746–55.
41. Chaabane F, Graf A, Jequier L, Coste AT. Review on Antifungal Resistance Mechanisms in the Emerging Pathogen *Candida auris*. *Front Microbiol*. 2019; 10:2788.
42. Pardo M, Monteoliva L, Vázquez P, Martínez R, Molero G, Nombela C, et al. PST1 and ECM33 encode two yeast cell surface GPI proteins important for cell wall integrity. *Microbiology (Reading, Engl)*. 2004; 150(Pt 12):4157–70. <https://doi.org/10.1099/mic.0.26924-0> PMID: 15583168
43. De Groot PWJ, Hellingwerf KJ, Klis FM. Genome-wide identification of fungal GPI proteins. *Yeast*. 2003; 20(9):781–96. <https://doi.org/10.1002/yea.1007> PMID: 12845604
44. De Groot PWJ, Kraneveld EA, Yin QY, Dekker HL, Gross U, Crielaard W, et al. The cell wall of the human pathogen *Candida glabrata*: differential incorporation of novel adhesin-like wall proteins. *Eukaryotic Cell*. 2008; 7(11):1951–64.
45. Hamada K, Terashima H, Arisawa M, Yabuki N, Kitada K. Amino acid residues in the omega-minus region participate in cellular localization of yeast glycosylphosphatidylinositol-attached proteins. *J Bacteriol*. 1999; 181(13):3886–9. <https://doi.org/10.1128/JB.181.13.3886-3889.1999> PMID: 10383953
46. Esher SK, Ost KS, Kohlbrenner MA, Pianalto KM, Telzrow CL, Campuzano A, et al. Defects in intracellular trafficking of fungal cell wall synthases lead to aberrant host immune recognition. *PLoS Pathog*. 2018; 14(6):e1007126. <https://doi.org/10.1371/journal.ppat.1007126> PMID: 29864141
47. Yin QY, De Groot PWJ, Dekker HL, De Jong L, Klis FM, De Koster CG. Comprehensive proteomic analysis of *Saccharomyces cerevisiae* cell walls: identification of proteins covalently attached via glycosylphosphatidylinositol remnants or mild alkali-sensitive linkages. *J Biol Chem*. 2005; 280(21):20894–901.
48. Klis FM, Mol P, Hellingwerf K, Brul S. Dynamics of cell wall structure in *Saccharomyces cerevisiae*. *FEMS Microbiol Rev*. 2002; 26(3):239–56.
49. Yakupova EI, Bobyleva LG, Vikhlyantsev IM, Bobylev AG. Congo Red and amyloids: history and relationship. *Biosci Rep*. 2019; 39(1). <https://doi.org/10.1042/BSR20181415> PMID: 30567726
50. Veelders M, Bruckner S, Ott D, Unverzagt C, Mosch HU, Essen LO. Structural basis of flocculin-mediated social behavior in yeast. *Proc Natl Acad Sci U S A*. 2010; 107(52):22511–6. <https://doi.org/10.1073/pnas.1013210108> PMID: 21149680

51. De Groot PWJ, De Boer AD, Cunningham J, Dekker HL, De Jong L, Hellingwerf KJ, et al. Proteomic analysis of *Candida albicans* cell walls reveals covalently bound carbohydrate-active enzymes and adhesins. *Eukaryot Cell*. 2004; 3(4):955–65.
52. Gomez-Molero E, De Boer AD, Dekker HL, Moreno-Martinez A, Kraneveld EA, Ichsan, et al. Proteomic analysis of hyperadhesive *Candida glabrata* clinical isolates reveals a core wall proteome and differential incorporation of adhesins. *FEMS Yeast Res*. 2015; 15(8).
53. Moreno-Martinez AE, Gomez-Molero E, Sanchez-Virosta P, Dekker HL, De Boer A, Eraso E, et al. High Biofilm Formation of Non-Smooth *Candida parapsilosis* Correlates with Increased Incorporation of GPI-Modified Wall Adhesins. *Pathogens*. 2021; 10(4).
54. De Groot PWJ, Brandt BW, Horiuchi H, Ram AFJ, De Koster CG, Klis FM. Comprehensive genomic analysis of cell wall genes in *Aspergillus nidulans*. *Fungal Genet Biol*. 2009; 46 Suppl 1:S72–81.
55. Navarro-Arias MJ, Hernandez-Chavez MJ, Garcia-Carnero LC, Amezcua-Hernandez DG, Lozoya-Perez NE, Estrada-Mata E, et al. Differential recognition of *Candida tropicalis*, *Candida guilliermondii*, *Candida krusei*, and *Candida auris* by human innate immune cells. *Infect Drug Resist*. 2019; 12:783–94.
56. Lenardon MD, Munro CA, Gow NA. Chitin synthesis and fungal pathogenesis. *Curr Opin Microbiol*. 2010; 13(4):416–23. <https://doi.org/10.1016/j.mib.2010.05.002> PMID: 20561815
57. Mora-Montes HM, Netea MG, Ferwerda G, Lenardon MD, Brown GD, Mistry AR, et al. Recognition and blocking of innate immunity cells by *Candida albicans* chitin. *Infect Immun*. 2011; 79(5):1961–70.
58. Cortes JC, Konomi M, Martins IM, Munoz J, Moreno MB, Osumi M, et al. The (1,3)beta-D-glucan synthase subunit Bgs1p is responsible for the fission yeast primary septum formation. *Mol Microbiol*. 2007; 65(1):201–17. <https://doi.org/10.1111/j.1365-2958.2007.05784.x> PMID: 17581129
59. Bhavsar-Jog YP, Bi E. Mechanics and regulation of cytokinesis in budding yeast. *Semin Cell Dev Biol*. 2017; 66:107–18. <https://doi.org/10.1016/j.semcdb.2016.12.010> PMID: 28034796
60. Hall RA, Lenardon MD, Alvarez FJ, Nogueira FM, Mukaremera L, Gow NAR. The *Candida albicans* Cell Wall: Structure and Role in Morphogenesis and Immune Recognition. In: Mora-Montes HM, editor. *The Fungal Cell Wall*: Nova Science Publishers, Inc; 2013.
61. Hoffmann D, Diderrich R, Reithofer V, Friederichs S, Kock M, Essen LO, et al. Functional reprogramming of *Candida glabrata* epithelial adhesins: the role of conserved and variable structural motifs in ligand binding. *J Biol Chem*. 2020; 295(35):12512–24. <https://doi.org/10.1074/jbc.RA120.013968> PMID: 32669365
62. Zupancic ML, Frieman M, Smith D, Alvarez RA, Cummings RD, Cormack BP. Glycan microarray analysis of *Candida glabrata* adhesin ligand specificity. *Mol Microbiol*. 2008; 68(3):547–59. <https://doi.org/10.1111/j.1365-2958.2008.06184.x> PMID: 18394144
63. Bouyx C, Schiavone M, Francois JM. FLO11, a Developmental Gene Conferring Impressive Adaptive Plasticity to the Yeast *Saccharomyces cerevisiae*. *Pathogens*. 2021; 10(11).
64. Bojsen RK, Andersen KS, Regenber B. *Saccharomyces cerevisiae*—a model to uncover molecular mechanisms for yeast biofilm biology. *FEMS Immunol Med Microbiol*. 2012; 65(2):169–82.
65. Ene IV, Heilmann CJ, Sorgo AG, Walker LA, De Koster CG, Munro CA, et al. Carbon source-induced reprogramming of the cell wall proteome and secretome modulates the adherence and drug resistance of the fungal pathogen *Candida albicans*. *Proteomics*. 2012; 12(21):3164–79. <https://doi.org/10.1002/pmic.201200228> PMID: 22997008
66. Heilmann CJ, Sorgo AG, Siliakus AR, Dekker HL, Brul S, De Koster CG, et al. Hyphal induction in the human fungal pathogen *Candida albicans* reveals a characteristic wall protein profile. *Microbiology (Reading)*. 2011; 157(Pt 8):2297–307. <https://doi.org/10.1099/mic.0.049395-0> PMID: 21602216
67. Sorgo AG, Heilmann CJ, Dekker HL, Bekker M, Brul S, De Koster CG, et al. Effects of fluconazole on the secretome, the wall proteome, and wall integrity of the clinical fungus *Candida albicans*. *Eukaryot Cell*. 2011; 10(8):1071–81. <https://doi.org/10.1128/EC.05011-11> PMID: 21622905
68. Albrecht A, Felk A, Pichova I, Naglik JR, Schaller M, De Groot P, et al. Glycosylphosphatidylinositol-anchored proteases of *Candida albicans* target proteins necessary for both cellular processes and host-pathogen interactions. *J Biol Chem*. 2006; 281(2):688–94.
69. De Groot PWJ, Brandt BW. ProFASTA: a pipeline web server for fungal protein scanning with integration of cell surface prediction software. *Fungal Genet Biol*. 2012; 49(2):173–9. <https://doi.org/10.1016/j.fgb.2011.12.009> PMID: 22230096
70. Eisenhaber B, Schneider G, Wildpaner M, Eisenhaber F. A sensitive predictor for potential GPI lipid modification sites in fungal protein sequences and its application to genome-wide studies for *Aspergillus nidulans*, *Candida albicans*, *Neurospora crassa*, *Saccharomyces cerevisiae* and *Schizosaccharomyces pombe*. *J Mol Biol*. 2004; 337(2):243–53.
71. Mirdita M, Ovchinnikov S, Steinegger M. ColabFold—Making protein folding accessible to all. *BioRxiv*. 2021.

72. Wang J, Youkharibache P, Zhang D, Lanczycki CJ, Geer RC, Madej T, et al. iCn3D, a web-based 3D viewer for sharing 1D/2D/3D representations of biomolecular structures. *Bioinformatics*. 2020; 36(1):131–5. <https://doi.org/10.1093/bioinformatics/btz502> PMID: 31218344
73. Holm L. Using Dali for Protein Structure Comparison. *Methods Mol Biol*. 2020; 2112:29–42. https://doi.org/10.1007/978-1-0716-0270-6_3 PMID: 32006276
74. Krissinel E, Henrick K. Secondary-structure matching (SSM), a new tool for fast protein structure alignment in three dimensions. *Acta Crystallogr D Biol Crystallogr*. 2004; 60(Pt 12 Pt 1):2256–68. <https://doi.org/10.1107/S0907444904026460> PMID: 15572779
75. Pardini G, De Groot PWJ, Coste AT, Karababa M, Klis FM, de Koster CG, et al. The CRH family coding for cell wall glycosylphosphatidylinositol proteins with a predicted transglycosidase domain affects cell wall organization and virulence of *Candida albicans*. *J Biol Chem*. 2006; 281(52):40399–411.
76. Thevissen K, De Mello Tavares P, Xu D, Blankenship J, Vandenbosch D, Idkowiak-Baldys J, et al. The plant defensin RsAFP2 induces cell wall stress, septin mislocalization and accumulation of ceramides in *Candida albicans*. *Mol Microbiol*. 2012; 84(1):166–80. <https://doi.org/10.1111/j.1365-2958.2012.08017.x> PMID: 22384976
77. Kapteyn JC, Hoyer LL, Hecht JE, Müller WH, Andel A, Verkleij AJ, et al. The cell wall architecture of *Candida albicans* wild-type cells and cell wall-defective mutants. *Mol Microbiol*. 2000; 35(3):601–11.
78. Li D, Williams D, Lowman D, Monteiro MA, Tan X, Kruppa M, et al. The *Candida albicans* histidine kinase Chk1p: signaling and cell wall mannan. *Fungal Genet Biol*. 2009; 46(10):731–41.